Biophys. Res. Commun. 115, 841-848.
Rius, F. X., Knowles, P. F., & Pettersson, G. (1984) *Biochem. J. 220*, 767-772.
Summers, M. C., Markovic, R., & Klinman, J. P. (1979) *Biochemistry 18*, 1969-1979.
Suzuki, S., Sakurai, T., Manabe, T., Okuyama, T. (1983) *Biochemistry 22*, 1630-1635.
Suzuki, S., Sakurai, T., Nakahara, A., Manabe, T., & Okuyama, T. (1986) *Biochemistry 25*, 338-341.
Tabor, C. W., Tabor, H., & Rosenthal, S. M. (1954) *J. Biol. Chem. 208*, 645-661.
Turini, P., Sabatini, S., Befani, O., Chimenti, F., Casanova, C., Riccio, P. L., & Mondovi, B. (1982) *Anal. Biochem. 125*, 294-298.
Yamada, H., & Yasunobu, K. T. (1962) *J. Biol. Chem. 237*, 1511-1566.
Yasunobu, K. T., Ishitaki, H., & Minamiura, N. (1976) *Mol. Cell. Biochem. 13*, 3-29.
Zeidan, H., Watanabe, K., Piette, L. H., & Yasunobu, K. T. (1980) *J. Biol. Chem. 255*, 7621-7626.

Structure–Function Studies of Substrate Oxidation by Bovine Serum Amine Oxidase: Relationship to Cofactor Structure and Mechanism†

Christa Hartmann‡ and Judith P. Klinman*
Department of Chemistry, University of California, Berkeley, Berkeley, California 94720
Received August 29, 1990; Revised Manuscript Received December 28, 1990

ABSTRACT: The chemical mechanism of substrate oxidation, catalyzed by bovine serum amine oxidase, has been explored by a detailed investigation of structure–reactivity correlations. Past mechanistic studies, involving the reductive trapping of substrate to cofactor [Hartmann, C., & Klinman, J. P. (1987) *J. Biol. Chem. 262*, 962], implied the intermediacy of a substrate imine complex in the catalytic redox mechanism. These studies led to the proposal of a transamination mechanism for substrate oxidation, analogous to pyridoxal phosphate dependent enzymes. In pyridoxal phosphate catalyzed reactions, the transamination process involves the transient formation of a resonance-stabilized carbanion intermediate. Although evidence has been presented describing the participation of an active site base in bovine serum amine oxidase catalysis [Farnum, M. F., Palcic, M. M., & Klinman, J. P. (1986) *Biochemistry 25*, 1898], the nature of the intermediate derived from C–H bond cleavage has not been directly addressed. To examine this question, a structure–reactivity study was performed using a series of para-substituted benzylamines. Having prior knowledge of the intrinsic isotope effect for an enzymatic reaction permits calculation of microscopic rate constants from steady-state data [Palcic, M. M., & Klinman, J. P. (1983) *Biochemistry 22*, 5957]. Deuterium isotope effects on k_{cat} and k_{cat}/K_m parameters were determined for all substrates, allowing for the calculation of rate constants for C–H bond cleavage (k_3) and substrate dissociation constants (K_d). Pre-steady-state constants obtained for *p*-acetylbenzylamine, *p*-(trifluoromethyl)benzylamine, and unsubstituted benzylamine exhibited excellent agreement with values calculated from steady-state isotope effects. Multiple regression analysis yielded an electronic effect of $\rho = 1.47 \pm 0.27$ for the bond cleavage step, supporting the intermediacy of a carbanion species. An additional effect, determined from regression analysis, indicated inhibition of catalysis by hydrophobic substituents ($\pi = -0.71 \pm 0.21$). These results lead to a reaction mechanism for amine oxidation by the covalently bound cofactor in bovine serum amine oxidase, 6-hydroxydopa [Janes, S. M., Mu, D., Wemmer, D., Smith, A. J., Kaur, S., Maltby, D., Burlingame, A. L., & Klinman, J. P. (1990) *Science 248*, 981].

Bovine serum amine oxidase (BSAO)[1] belongs to the class of proteins designated copper amine oxidases. These proteins catalyze a spectrum of activities, which include the cross-linking of collagen and elastin (Siegel, 1979) and the regulation of intracellular polyamines (Bachrach, 1985). Although the precise function of the plasma amine oxidases is unknown, their broad specificity suggests a role in the regulation of blood plasma biogenic amines (Buffoni, 1966).

In addition to active site copper, the copper amine oxidases contain a covalently bound carbonyl cofactor capable of forming chromophoric derivatives with phenylhydrazines. The pursuit of detailed mechanistic studies of these proteins has been hampered by the absence of a confirmed structure for the active site cofactor. In fairly recent studies, Ameyama et al. (1984) and Lobenstein-Verbeek et al. (1984) proposed that the active site cofactor in BSAO was a pyrroloquinoline quinone (PQQ), a tricyclic quinone previously demonstrated to exist in a number of prokaryotes (Duine et al., 1987). However, new studies by Janes et al. (1990) show very clearly that the active site cofactor is a dihydroxy derivative of tyrosine, referred to as 6-hydroxydopa or topa.

Model studies of topa indicate that the reduced form [Figure 1 (**1**)] is quite unstable (Janes et al., 1990), undergoing rapid

†This work was supported by a grant to J.P.K. from the National Institutes of Health (GM 39296).
*Author to whom correspondence should be addressed.
‡Present address: Department of Pharmaceutical Chemistry, University of California, San Francisco, CA 94143.

[1] Abbreviations: BSAO, bovine serum amine oxidase; UCB, University of California, Berkeley; NMR, nuclear magnetic resonance; PQQ, pyrroloquinoline quinone; THF, tetrahydrofuran; DME, ethylene glycol dimethyl ether.

0006-2960/91/0430-4605$02.50/0

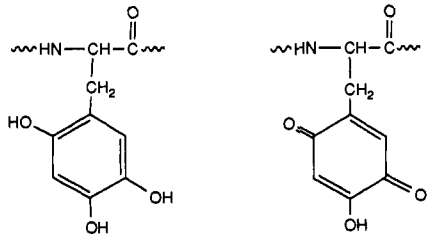

1 2

FIGURE 1: Structures of the active site cofactor in bovine serum amine oxidase: **1**, the reduced form of topa; **2**, topa quinone, illustrated as the *p*-quinone. In solution, an equilibrium mixture of *o*- and *p*-quinone is expected.

air oxidation to a quinone (**2**). The presence of a quino structure in BASO is compatible with previous inactivation experiments, which indicated an incorporation of carbon-14, but *not* tritium, into enzyme reduced by [^{3}H]$NaCNBH_4$ in the presence of [^{14}C]benzylamine (Hartmann & Klinman, 1987). Although this result was originally discussed in the context of the *o*-quinone of PQQ, it is equally compatible with a *p*-quinone structure [Figure 1 (**2**)]. As originally noted (Hartmann & Klinman, 1987), reductive trapping of substrate onto cofactor with $NaCNBH_3$ implies the intermediacy of a substrate imine complex in the catalytic redox mechanism. The recent demonstration that nitrogen is transferred from substrate to cofactor following anaerobic incubation of BSAO with benzylamine further implicates covalent species, in this case a product imine complex as precursor to aldehyde and the aminoquinol form of cofactor [Janes and Klinman, (preceding paper in this issue)].

The above-described properties of the BSAO reaction have led to the proposal of a transamination mechanism for substrate oxidation (Klinman et al., 1988). By analogy to the better studied pyridoxal phosphate dependent enzymes, such a transamination process is expected to be base catalyzed and to lead to the transient formation of a resonance-stabilized carbanion intermediate. Although evidence has been presented for base-catalyzed processes at the BSAO active site (Farnum et al., 1986), the mechanism of C–H cleavage during substrate oxidation has not been previously addressed. In the present study we have conducted a detailed investigation of structure–reactivity correlations in the BSAO-catalyzed oxidation of a series of ring-substituted benzylamines, providing evidence for proton removal in the course of substrate oxidation. These results allow us to write a reaction mechanism for amine oxidation by the new redox cofactor topa.

Experimental Procedures

Materials

All chemicals were of reagent grade and were used without further purification unless otherwise specified. 4-Bromobenzonitrile, 4-(dimethylamino)benzonitrile, 4-fluorobenzonitrile, 4-acetylbenzonitrile, 4-methoxybenzonitrile, 4-cyanophenol, ethylene glycol, and $LiAlD_4$ (isotopic purity >98%) were obtained from Aldrich. Benzonitrile was from Matheson, Coleman and Bell, 4-(trifluoromethyl)benzonitrile and $LiAlH_4$ were from Alfa Ventron, 4-isopropylbenzoic acid was from Sigma, 4-methylbenzonitrile was from Trans World Chemicals, and benzyl bromide was from Fluka AG Chemicals. Dimethylformamide (DMF) and ethylene glycol dimethyl ether (DME) were freshly distilled immediately prior to use.

Methods

Enzyme activity was assayed spectrophotometrically with 10 mM benzylamine as substrate in 100 mM phosphate buffer, pH 7.2, by monitoring the increase in absorbance at 250 nm corresponding to benzaldehyde formation. The difference in extinction coefficient of benzaldehyde vs benzylamine was taken as 12800 M^{-1} cm^{-1} (Neumann et al., 1975). The protein concentration was determined spectrophotometrically at 280 nm by using $E^{1\%}_{1cm}$ of 20.8 (Yasunobu et al., 1976).

Melting points (Pyrex capillary) were uncorrected. UV spectra were determined with a Cary Model 118 ultraviolet–visible spectrophotometer. ^{1}H NMR spectra were determined on a Varian EM-390 (90 MHz) or University of California, Berkeley (UCB), spectrophotometers (200 MHz; 250 MHz). Chemical shifts (in ppm) were obtained relative to internal standards of sodium 2,2-dimethyl-2-silapentane-5-sulfonate or tetramethylsilane. Elemental analyses were performed by the Analytical Laboratory, UCB. Mass spectral data, tabulated as *m/z*, were obtained from either the Mass Spectrometry Center, College of Chemistry, UCB, or the Midwest Center for Mass Spectrometry, Department of Chemistry, University of Nebraska, Lincoln. Oxygen uptake assays were performed with a Yellow Springs Instrument polargraphic oxygen electrode, Model 53.

Synthesis of Para-Substituted Benzylamine Hydrochlorides. The syntheses of C-1-protonated and -dideuterated benzylamine and all other para-substituted benzylamines, except where noted (cf. supplementary material), were carried out in parallel by the reduction of the corresponding nitrile with $LiAlH_4$ or $LiAlD_4$ under nitrogen atmosphere according to a modification of the method of Nystrom (1955). In a typical synthesis, 0.026 mol of the corresponding benzonitrile dissolved in 70 mL of ether was added dropwise to a suspension of 0.078 mol of $LiAlH_4$ (or $LiAlD_4$) in 50 mL of ether over a period of 1 h. The reaction mixture was stirred for an additional hour. Water (5–7 mL) was added cautiously to quench the reaction, and the solution was acidified with 45 mL of 3 M H_2SO_4 and 35 mL of water, extracted with ether, washed with water, and dried over anhydrous sodium sulfate. Gaseous hydrochloric acid was bubbled through the combined ethereal extracts to form the HCl salt. The precipitate was filtered and recrystallized from methanol/water. Final yields were characteristically between 80% and 95% of the theoretical yields and are not individually noted for the one-step $LiAlH_4$ reductions.

^{1}H NMR spectra of all dideuterated samples were determined with a Varian EM-390 or UCB-200/250 spectrometers with D_2O as solvent and showed no detectable signal attributable to the methylene protons, indicating less than 2% contamination by nondeuterated material. The melting points of all synthesized substrates and mixtures of synthesized and authentic materials (when available) were identical. Mass spectral analyses of all synthesized hydrochlorides showed the expected *m/z* for the parent ions after loss of HCl. The syntheses of *p*-OH-, *p*-$(CH_3)_2CH$-, and *p*-CH_3CO-benzylamines required either protection/deprotection steps (*p*-OH and *p*-CH_3CO) or synthetic routes different from that outlined above [*p*-$(CH_3)_2CH$]. Details of these reactions are available in the supplementary material.

Pre-Steady-State Kinetics. The stopped-flow apparatus was prepared for anaerobiosis by overnight incubation with a solution of 100 mM glucose, 50 units/mL glucose oxidase, and 50 units/mL catalase in 100 mM potassium phosphate buffer, pH 7.2. Anaerobic buffer, containing the same components as above, was used to flush the syringes and chamber immediately prior to use.

For the reductive half-reaction, the anaerobic enzyme was prepared in a tonometer and contained 50–60 μM enzyme in

Table I: Comparison of k_{cat}, $^{D}(k_{cat})$, k_{cat}/K_m, and $^{D}(k_{cat}/K_m)$ Values for Para-Substituted Benzylamines[a]

X	k_{cat}(H) (s^{-1})	k_{cat}(D) (s^{-1})	$^{D}(k_{cat})$	k_{cat}/K_m(H) (mM^{-1} s^{-1})	k_{cat}/K_m(D) (mM^{-1} s^{-1})	$^{D}(k_{cat}/K_m)$
H	0.564 ± 0.005	0.149 ± 0.026	3.77 ± 0.48	0.414 ± 0.0617	0.0277 ± 0.0006	14.9 ± 6.0
Br	1.40 ± 0.25	0.317 ± 0.018	4.42 ± 0.81	4.50 ± 0.50	0.551 ± 0.061	8.17 ± 0.97
F	2.69 ± 0.27	1.11 ± 0.17	2.42 ± 0.25	3.77 ± 0.25	0.651 ± 0.054	5.79 ± 0.19
CF_3	1.92 ± 0.13	0.914 ± 0.079	2.10 ± 0.18	6.49 ± 0.74	1.15 ± 0.13	5.64 ± 0.48
CH_3	0.444 ± 0.049	0.0943 ± 0.0261	4.71 ± 0.24	0.415 ± 0.050	0.0526 ± 0.0052	7.89 ± 0.98
$N(CH_3)_2$	0.0260 ± 0.0014	0.0154 ± 0.0008	1.69 ± 0.002	0.178 ± 0.044	0.0120 ± 0.0019	14.8 ± 3.8
OCH_3	0.974 ± 0.050	0.588 ± 0.045	1.66 ± 0.004	17.1 ± 3.7	1.49 ± 0.17	11.5 ± 2.5
$CH(CH_3)_2$	0.279 ± 0.010	0.0278 ± 0.0017	10.0 ± 0.01	1.54 ± 0.10	0.112 ± 0.013	13.8 ± 1.0
OH	0.944 ± 0.028	0.0541 ± 0.075	1.74 ± 0.06	5.29 ± 0.42	0.564 ± 0.049	9.38 ± 0.62
$COCH_3$	1.18 ± 0.056	0.998 ± 0.066	1.18 ± 0.08	7.64 ± 0.96	1.18 ± 0.15	6.47 ± 0.66

[a] Values reflect the average of 2–4 kinetic analyses.

100 mM potassium phosphate buffer, pH 7.2, 100 mM glucose, 50 units/mL glucose oxidase, and 50 units/mL catalase. Substrate solutions were prepared for anaerobiosis by bubbling high-purity argon through 8 mL of the phosphate/glucose buffer in 10 mL of disposable syringes for 15 min, followed by addition of 50 units/mL each of glucose oxidase and catalase. The activity of the enzyme remained unchanged after the experiments were completed, relative to initial measurements.

The anaerobic reduction of plasma amine oxidase by excess amine substrates was monitored by following the decrease in absorbance at 480 nm as a function of time. A total of 1024 data points were collected and stored. First-order rate constants were calculated as described by Ramsey et al. (1986) by using a program from Anarac Associates (1987). Four determinations of the rate constants for each substrate were performed and averaged to obtain the final rate parameters with associated standard deviations.

Steady-State Kinetics. Initial velocity studies for both deuterated and protonated substrates were carried out 25 °C in 100 mM potassium phosphate buffer, pH 7.2. Substrate solutions were freshly prepared immediately prior to use. The rate of reaction was measured by monitoring the oxygen consumption of air-saturated solutions. Velocities for both the protio and dideuterio substrates were obtained on the same day. All data were fitted to the expression

$$v/E_T = V_{max}[S]/(K_m + S) \quad (1)$$

by using the FORTRAN program of Cleland (1979), which was translated to BASIC by N. G. Ahn for use on a Northstar Horizon computer. Enzyme activity was normalized to 0.36 unit/mg, and microscopic rate constants and dissociation constants were calculated from the eqs 5 and 6 in the text, using the data for k_{cat}, $^{D}(k_{cat})$, k_{cat}/K_m, and $^{D}(k_{cat}/K_m)$ shown in Table I. The units for k_{cat} and k_{cat}/K_m are s^{-1} and mM^{-1} s^{-1}, respectively. Propagated errors were calculated according to Palcic and Klinman (1983).

Results

Steady-State Kinetic Parameters for the BSAO-Catalyzed Oxidation of Para-Substituted Benzylamines. The BSAO-catalyzed oxidation of a series of ring-substituted [1,1-^{1}H]- and [1,1-^{2}H]benzylamines was studied under steady-state conditions. The resulting parameters are summarized in Table I. Although reactions were run at a single oxygen concentration (0.2 mM), this is ca. 15-fold larger than K_m (14 μM with benzylamine as the substrate), assuring that kinetic values reflect saturation by oxygen. With the exception of the dimethylamino substituent, ring substitution has a modest effect on k_{cat}(H), ranging from a low value of 0.279 s^{-1} for *p*-$(CH_3)_2CH$ to a maximum value of 2.69 s^{-1} for the *p*-F substituent. The effect of substituent increases upon substrate deuteration, such that k_{cat}(D) shows a range of 0.0278–1.11 s^{-1} in proceeding from *p*-$(CH_3)_2CH$- to *p*-F-benzylamine. This increased dependence on substrate structure for cleavage of a C–D vs a C–H bond is due to differences in rate limitation by substrate oxidation, as reflected in the relative magnitudes of isotope effects, $^{D}(k_{cat})$ (Table I).

It can be seen (Table I) that k_{cat}/K_m indicates a different dependence on substituent from k_{cat}, with *p*-$(CH_3)_2N$-benzylamine indicating the slowest rate and *p*-CH_3O-benzylamine the fastest rate. Once again, oxidation of deuterated substrate alters relative reactivity, but to a lesser extent than with k_{cat}, reflecting a smaller range in isotope effects, $^{D}(k_{cat}/K_m)$ (Table I). These differing trends in kinetic parameters with changes in substrate structure are a direct consequence of kinetic complexity, indicating the need to evaluate constants for individual steps before mechanistically significant conclusions can be reached.

Calculation of Rate and Dissociation Constants from Steady-State Parameters. In an early study of [1,1-$^2H_2$]-benzylamine oxidation, the magnitude of the deuterium isotope was shown to be very large under conditions of both steady-state and pre-steady-state kinetics, $^{D}(k) = 13.5 \pm 1.3$, attributed to an intrinsic value for the hydrogen abstraction step (Palcic & Klinman, 1983). This value for $^{D}(k)$ has recently been confirmed in studies of primary and secondary tritium isotope effects (Grant & Klinman, 1989). As described (Palcic & Klinman, 1983), the availability of an intrinsic isotope effect can be used with experimental data for $^{D}(k_{cat})$ and $^{D}(k_{cat}/K_m)$ to obtain individual rate and binding constants in a complex kinetic mechanism.

In the case of BSAO, a minimal mechanism has been derived from existing kinetic data, eqs 2–4, where E_{ox} and E_{red} represent oxidized and reduced forms of enzyme, respectively (Palcic & Klinman, 1983). According to this minimal

$$E_{ox} + RCH_2NH_3^+ \underset{k_2}{\overset{k_1}{\rightleftharpoons}} E_{ox}{\cdot}RCH_2NH_3^+ \underset{k_4}{\overset{k_3}{\rightleftharpoons}} E_{red}{-}N^+H{=}CHR \quad (2)$$

$$E_{red}{-}N^+H{=}CHR \xrightarrow[H_2O]{k_5} E_{red}{-}NH_2 + RCHO \quad (3)$$

$$E_{red}{-}NH_2 \xrightarrow[O_2]{k_7} E_{ox} + H_2O_2 + NH_4^+ \quad (4)$$

mechanism, the BSAO reaction contains six unknowns (k_1, k_2, k_3, k_4, k_5, k_7) whereas steady-state studies with isotopically labeled substrates yield only four equations [k_{cat}, $^{D}(k_{cat})$, k_{cat}/K_m, $^{D}(k_{cat}/K_m)$]. Thus, even with a knowledge of an intrinsic isotope effect it is not possible to solve for each rate constant in the overall mechanism. However, Palcic and Klinman (1983) recognized that when the equilibrium isotope

Table II: Calculated Values for Individual Constants[a]

X	k_3 (s^{-1})	K_d (mM)
H	2.55 ± 0.67	6.84 ± 2.2
Br	5.12 ± 0.70	0.541 ± 0.106
F	23.7 ± 3.4	3.41 ± 1.13
CF_3	21.8 ± 2.2	1.25 ± 0.15
CH_3	1.49 ± 0.28	1.99 ± 0.37
$N(CH_3)_2$	0.470 ± 0.068	2.92 ± 0.65
OCH_3	18.4 ± 2.1	0.906 ± 0.218
$CH(CH_3)_2$	0.388 ± 0.048	0.232 ± 0.033
OH	15.9 ± 2.7	2.02 ± 0.76
$COCH_3$	81.9 ± 2.1	4.69 ± 1.27

[a] Average values from calculations of these constants for each kinetic measurement of $^D(k_{cat})$ and $^D(k_{cat}/K_m)$. Calculation of k_3 from eq 5 and K_d from eq 6 in text.

effect for the interconversion of E_{ox}·$RCH_2NH_3^+$ and E_{red}—NH^+=CHR is close to unity or when the partitioning of E_{red}—NH^+=CHR toward E_{red}—NH_2 and RCHO is very favorable, rate and isotope effect expressions reduce to

$$k_3 = \frac{k_{cat}[^D(k) - 1]}{^D(k_{cat}) - 1} \quad (5)$$

$$K_d = \frac{K_m[^D(k_{cat}/K_m) - 1]}{^D(k_{cat}) - 1} \quad (6)$$

Since one or both of these conditions is expected to pertain in the BSAO reaction, k_3, the rate constant for substrate oxidation, and K_d, the dissociation constant for substrate binding, can be obtained in a straightforward manner from kinetically accessible parameters and the intrinsic isotope effect on k_3, $^D(k)$. A surprising feature of eq 6 is the availability of K_d from a kinetically complex reaction without prior knowledge of the intrinsic isotope effect (Klinman & Matthews, 1985).

Values for k_3 and K_d have been computed from the data in Table I and are summarized in Table II. Although the calculation of k_3 for ring-substituted benzylamines rests on the assumption that $^D(k)$ is 13.5 for all benzylamines, anaerobic stopped-flow studies indicate deuterium isotope effects for *p*-(trifluoromethyl)benzylamine and *p*-acetylbenzylamine similar to those seen with benzylamine (cf. the discussion below and Table III). A second factor in the applicability of eqs 5 and 6 is the magnitude of $^D(k_{cat}/K_m)$ and $^D(k_{cat})$, with values close to unity leading to indeterminate results. In the case of BSAO, this is only a potential problem with *p*-CH_3CO-benzylamine, where $^D(k_{cat})$ is observed to be almost within experimental error of 1. However, a close correspondence is observed when comparing computed constants for *p*-CH_3CO-benzylamine to those measured under conditions of anaerobic stopped-flow kinetics (see below).

Anaerobic Stopped-Flow Kinetics. Under anaerobic conditions, the reduction of BSAO by benzylamine has previously been shown to lead to a single first-order decay in absorbance at 480 nm, attributed to reduction of cofactor, eq 2. Since imine hydrolysis, eq 3, appears to be quite rapid for this substrate, i.e., $k_5 \gg k_4$ (Farnum et al., 1986), the species being detected in the stopped flow is actually E_{red}—NH_2, rather than E_{red}—NH^+=CHR. In any case, the difference in absorbance between these two enzyme species is expected to be small, relative to differences between substrate and product imines, E_{ox}=NH^+CH_2R and E_{red}—NH^+=CHR, respectively. The reduction of enzyme by *p*-CF_3-benzylamine appeared very similar to that of benzylamine (Palcic & Klinman, 1983), both in absorbance vs time traces and in reciprocal plots of k_{obs} vs substrate concentration. Analysis of slopes and intercepts from

Table III: Anaerobic Stopped-Flow Parameters for Benzylamine, *p*-(Trifluoromethyl)benzylamine, and *p*-Acetylbenzylamine

substrate	k_3 (s^{-1})	$^D(k_3)$	k_3/K (mM^{-1} s^{-1})	$^D(k_3/K)$
benzylamine	2.28 ± 0.15	–[a]	4.85 ± 0.02	–[a]
p-CF_3-benzylamine	33.0 ± 1.5	11.4 ± 0.8	14.5 ± 1.1	8.75 ± 0.45
p-CH_3CO-benzylamine[b]	87.4 ± 1.8	11.3 ± 0.2	2.88 ± 0.03	2.41 ± 0.82

[a] Not determined. [b] Initial plots of $1/k_{obs}$ vs $1/S$ were curved. Analysis of data according to Strickland et al. (1975) (cf. Figure 3) yielded the summarized parameters.

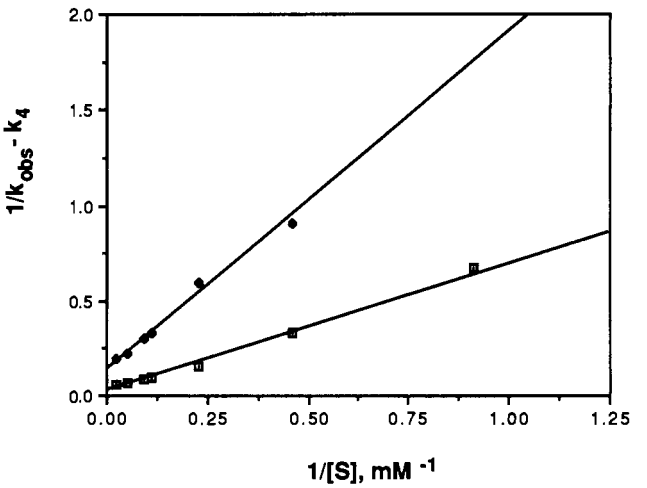

FIGURE 2: Reciprocal plot of corrected rate constants ($k_{obs} - k_4$) vs amine concentration for the pre-steady-state reduction of bovine serum amine oxidase by *p*-acetylbenzylamine. k_{obs} is the observed rate constant, and k_4 is the rate constant for formation of E·S from E·P (cf. eq 2 in text). The magnitude of k_4 was estimated from the intercept of a plot of k_{obs} vs [S]. (□) Protonated amine. (◆) Deuterated amine.

reciprocal plots for [1,1-^{1}H] and [1,1-^{2}H] substrates led to k_3, $^D(k_3)$, k_3/K, and $^D(k_3/K)$ (Table III), where K is a kinetic constant reflecting substrate binding and enzyme reduction. The reduction of enzyme by *p*-CH_3CO-benzylamine was found to be more complicated than for *p*-CF_3-benzylamine, such that initial plots of $1/k_{obs}$ vs $1/S$ were curved. As discussed by Strickland et al. (1975), nonlinear plots of this nature imply that the back rate for formation of E·S is finite, where the magnitude of this process can be measured from the *y*-intercept of plots of k_{obs} vs substrate concentration. Using this approach, we have estimated k_4 as 1.25 and 0.102 s^{-1} for protonated and deuterated substrates, respectively. Subsequent plots of $1/(k_{obs} - k_4)$ vs $1/S$ (Figure 2) provided the parameters summarized in Table III.

Two features of Table III are noteworthy. First, the isotope effects on k_3 for *p*-CF_3- and *p*-CH_3CO-benzylamines are very close to values previously reported for benzylamine (Palcic & Klinman, 1983)). Second, the experimentally determined values for k_3 are within 6% (*p*-CH_3CO-) and 34% (*p*-CF_3-) of computed values (Table II). Both of these observations support the validity of k_3 values calculated from steady-state parameters and $^D(k)$. This result is of particular interest in the case of the *p*-CH_3CO substrate, where stopped-flow studies indicate a reversal of the C–H cleavage step. As discussed above, the calculation of k_3 according to eq 5 requires either that k_4 is zero or that $^D(K_{eq}) = 1$. Since k_4 is nonzero for this substrate, we conclude that $^D(K_{eq})$ must be close to unity and, hence, that the substrate-derived hydrogen does not undergo significant exchange with solvent.[2] A similar conclusion,

Table IV: Parameter Colinearity[a]

	σ_p	π	E_s	V_w
σ_p	1.0			
π	0.127	1.0		
E_s	0.167	0.450	1.0	
V_w	0.098	0.388	0.616	1.0

[a] Correlation coefficients (squared), obtained from least-squares analysis of pairs of parameters.

regarding a sequestration of the substrate-derived hydrogen from solvent, had been reached earlier from studies of isotope effects with phenethylamine derivatives (Farnum & Klinman, 1986).

Comparison of experimentally determined K_d values to computed parameters is somewhat more difficult than with k_3, since the magnitude of $^D(k_3/K)$ in Table III is less than $^D(k_3)$. This indicates that stopped-flow data do not provide substrate dissociation constants directly. On the other hand, if we assign $k_3/K = k_1k_3/(k_2 + k_3)$, then $^D(k_3/K) = [^D(k_3) + k_3/k_2]/(1 + k_3/k_2)$; from these these two expressions, $k_2/k_1 = K_d$ values can be calculated to be 1.7 mM and 4.1 mM for p-CF_3- and p-CH_3CO-benzylamines, respectively. Once again, comparison of these numbers with values in Table II indicates agreement within 26% (p-CF_3) and 14% (p-CH_3CO).

Discussion

Multiple Linear Regression Analyses. With the availability of individual constants for substrate binding and oxidation (Table II), it becomes possible to pursue structure–reactivity correlations in a mechanistically relevant manner. A major goal of these studies has been to discern the mechanism of C–H bond cleavage from the dependence of k_3 on the electronic substituent. However, as noted previously (Klinman, 1976; Miller & Klinman, 1985), the study of structure–reactivity correlations in enzymology is complicated by the potential appearance of hydrophobic and steric interactions between ring substituents and active site residues. The contribution of each of these factors to a kinetic constant can be evaluated independently, given a choice of substituents which minimizes parameter colinearity. Evaluating the 10 substituted benzylamines used in the present study for such colinearity leads to the results in Table IV. As can be seen, there is no significant overlap between the electronic property of these substituents (σ_p) and either their hydrophobicity (π) or size (E_s and V_w). The only substantial colinearity appears in the correlation of E_s with V_w, which is to be expected since both of these represent steric parameters.

Multiple regression analyses have followed previous published protocols (Klinman, 1976; Miller & Klinman, 1985), utilizing the basic equation

$$\log (k_3, K_d) = \sigma_pA + \pi B + E_s(V_w)C + D \qquad (7)$$

where the magnitude of A, B, and C indicate the extent to which rate and dissociation constants depend on electronic, hydrophobic, and steric factors, respectively. We note that the choice of a steric parameter (E_s vs V_w) is not straightforward and will depend on the nature of the substrate binding pocket. The Taft steric parameter, E_s, reflects the van der Waals radius of the first atom of a substituent, implying that branched substituents can alter their conformation to minimize interactions with active site residues. By contrast, Bondi's treatment for calculated van der Waals radii correlates the total bulk of a given substituent (Bondi, 1964). The effects of both steric parameters have been evaluated in the present study.

Analyses were conducted on variations of eq 7 using either single- or two-parameter fits. A full three-parameter fit was considered incompatible with the size of the data set. In initial analyses, all of the data in Table II were utilized. However, the p-CH_3O substituent routinely displayed behavior that was aberrant relative to the other substituents. Preliminary pre-steady-state data on this substrate also appeared abnormal, providing evidence for the formation of an as yet unidentified intermediate. We therefore restricted our multiple-regression analyses to the remaining nine substrates in Table II. The best one- and two-parameter fits for k_3 and K_d are summarized below (eqs 8–11), where F relates the variance of the null hypothesis to the variance of each correlation. $F_{(0.99)}$ has been obtained from statistical tables and represents a lower limit of F for the correlation to be significant at the 99% level. For two-parameter equations, $F_x = F_{2,6}$ is the test for the significance of adding the indicated variable to the previous one-parameter equation and is interpreted by the corresponding t value, which is the probability that the coefficient of the added variable is zero.

rate of C–H bond cleavage

$$\log k_3 = 1.35(\pm0.51)\sigma + 0.71(\pm0.21) \qquad (8)$$
$$F_{1,7} = 7.08 \qquad F_{1,7(0.99)} = 12.3$$

$$\log k_3 = 1.47(\pm0.27)\sigma - 0.71(\pm0.12)\pi + 0.95(\pm0.12) \qquad (9)$$
$$F_{2,6} = 21.4 \qquad F_{2,6(0.99)} = 8.02 \qquad t = 0.002(\sigma);\ 0.075(\pi)$$

substrate dissociation constant

$$\log K_d = -0.52(\pm0.14)\pi + 0.42(\pm0.10) \qquad (10)$$
$$F_{1,7} = 13.9 \qquad F_{1,7(0.99)} = 12.3$$

$$\log K_d = 0.09(\pm0.25)\sigma - 0.52(\pm0.15)\pi + 0.42(\pm0.11) \qquad (11)$$
$$F_{2,6} = 6.16 \qquad F_{2,6(0.99)} = 8.02$$
$$t = 0.721(\sigma);\ 0.013(\pi) \qquad (11)$$

For the C–H bond cleavage step, the data correlate with σ_p between the 95% and 99% level, eq 8. The best two-parameter correlation for k_3 includes π as well as σ_p. As shown in eq 9, this additional parameter yields a statistically improved fit, with a small, 7.5%, probability ($t = 0.075$) that the coefficient B of π is zero. With regard to substrate binding, the single parameter which yielded a significant fit was π, eq 10. The best two-parameter fit for binding included σ_p, eq 11, but even in this instance the statistical improvement was insignificant ($t = 72\%$). It should be noted that no correlation was seen in the analysis of both k_3 and K_d with either E_s or V_w.

Correlation of Structure and Mechanism. As indicated from eqs 10 and 11, the sole determinant of relative substrate binding is substituent hydrophobicity, implying the presence of a lipophilic binding pocket at the active site of BSAO. It is particularly interesting that the same effect of hydrophobicity appears in the two-parameter fit for k_3. This indicates that while hydrophobic interactions are favorable for binding, they *impede* catalysis. A simple explanation for this result may lie with the fact that phenethylamines, rather than benzylamines, are the physiologically relevant substrates for BSAO. We suggest that the smaller benzylamine substrates bind to a hydrophobic cavity in such a way as to prevent effective interaction with the active site cofactor and base. Only upon movement of the para substituent out of the hy-

[2] In the event that the substrate-derived hydrogen exchanged with solvent, $K_{eqH} = k_{3H}/k_{4H}$, but $K_{eqD} = k_{3D}/k_{4H}$. Under this condition, $^D(K_{eq}) = k_{3H}/k_{3D}$.

Scheme I: Proposed Reaction Mechanism for Bovine Serum Amine Oxidase[a]

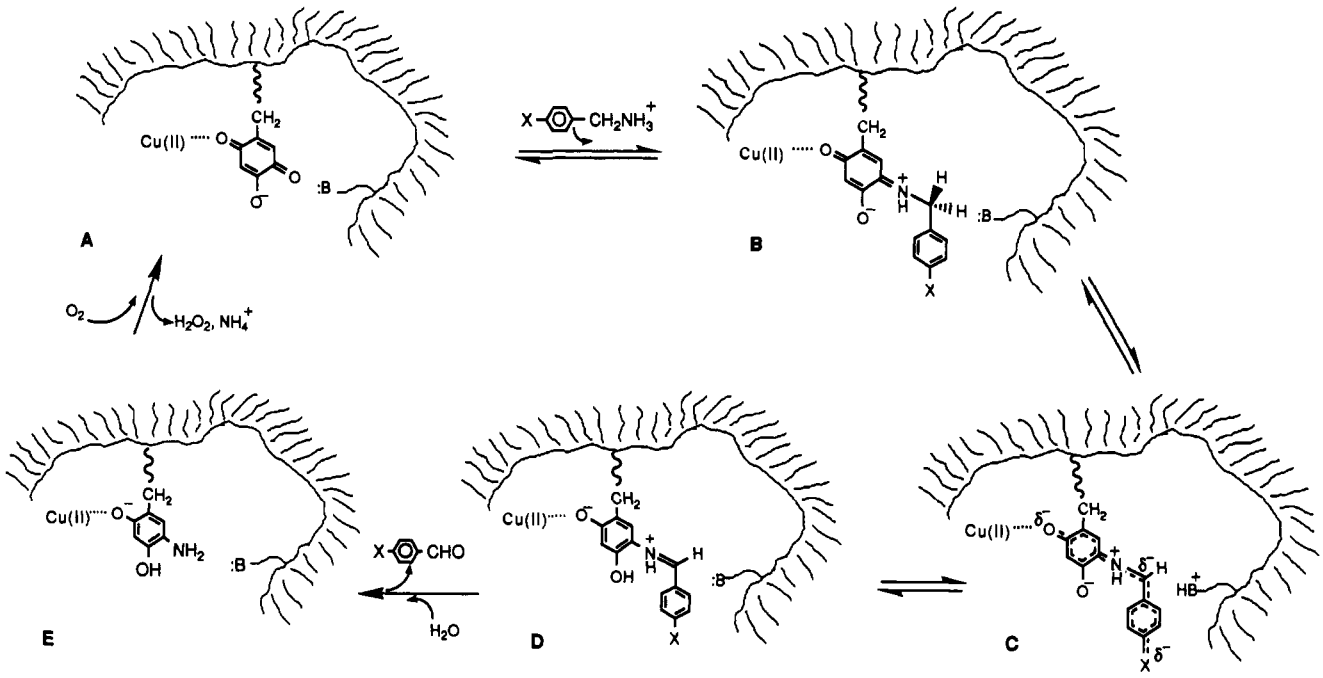

[a] (A) The active site cofactor, topa quinone, shown in proximity to an active site base and copper atom. (B) The covalent imine complex between substrate and cofactor, generated subsequent to simple E·S complex formation. (C) The carbanion intermediate, generated upon proton transfer from substrate to the active site base. (D) Product imine complex, in which the substrate-derived proton has been transferred to the oxyanion at C-4 of cofactor. (E) The aminoquinol of cofactor, formed by hydrolysis of aldehyde from the product imine complex. As discussed by Janes and Klinman (preceding paper in this issue), steady-state oxidation of species E is expected to form a transient iminoquinone species, which may undergo either direct hydrolysis to species A (as shown) or a transimination reaction with substrate to generate species B.

drophobic site is it possible for covalent attachment to cofactor and subsequent C–H bond cleavage.

Figure 3B shows the adjusted correlation of $\log k_3 + 0.71\pi$ vs σ_p, for comparison to the simpler fit of $\log k_3$ vs σ_p (Figure 3A). From the slope of Figure 3B, we obtain a ρ value of 1.47 ± 0.27 for the C–H bond cleavage step. The positive slope of this correlation, indicating a significant rate enhancement by electron-withdrawing substituents, implicates a proton activation mechanism. In Scheme I, we have integrated this fact with previous recent findings in the BSAO reaction. As illustrated, the active site cofactor is 6-hydroxydopa (topa) (Janes et al., 1990). Subsequent to initial complex formation, covalent attachment of substrate to the C-3 carbonyl of cofactor leads to a Schiff base intermediate, species B in Scheme I, which can be trapped by cyanoborohydride reduction (Hartmann & Klinman, 1987). Subsequent, base-catalyzed hydrogen abstraction leads to a carbanionic intermediate, with the resulting negative charge undergoing partial delocalization into the substituted benzene ring of substrate and into the substituted benzene ring of cofactor. Hydrolysis of the product Schiff base complex is proposed to be facilitated by proton transfer from the active site base to the oxyanion at position 4 of cofactor, species D in Scheme I. This proton transfer would free up the active site base for subsequent catalysis of a tritium exchange reaction at the β-carbon of phenethylamine derivatives [cf. Lovenberg and Beaven (1971)]. It would also serve to destabilize the product Schiff base complex, giving rise to a rapid hydrolysis reaction (Farnum et al., 1986), which results in nitrogen transfer from substrate to cofactor [Janes and Klinman (preceding paper in this issue)] to product species E. Although the reoxidation of reduced cofactor has not yet been studied and characterized, this process is proposed to be facilitated by active site copper. We have placed an active site copper adjacent to the oxygen at C-6 of cofactor (Scheme I), as this appears consistent with distance mapping experiments by Williams and Falk (1986) on the pig plasma enzyme.

Our conclusion of a proton activation mechanism in the BSAO-catalyzed oxidation of substrate is fully consistent with previous studies of BSAO. For example, Neumann et al. (1975) demonstrated an enzyme-catalyzed production of phenacetaldehyde from β-chlorophenethylamine. Aldehyde was proposed to arise from a base-catalyzed elimination of HCl from β-chlorophenethylamine to form an enamine intermediate, followed by tautomerization to imine and hydrolysis to phenacetaldehyde and ammonia. Additional, early evidence for a proton abstraction type mechanism followed from the observations of Lovenberg and Beaven (1971) that BSAO catalyzes an exchange reaction from the β-carbon of phenethylamine substrates. As a result of pH-dependent and sterochemical studies of this exchange process, a single base of pK_a = 5.2–5.5 has been postulated to catalyze both substrate oxidation (at C-1) and triton exchange (at C-2) (Farnum et al., 1986; Farnum & Klinman, 1986).

Although the above discussion has focused on the use of an active site side chain as the catalytic base, we had also considered the oxyanion at C-4 of cofactor as a possible, proton-abstracting species. After some reflection, however, the latter mechanism was concluded to be highly unlikely. First, transfer of hydrogen from substrate to oxygen at position 4 of cofactor would require that the incipient carbanion at C-1 of substrate be oriented within the plane of the cofactor ring. Such a geometry would impede carbanion delocalization into the electron-stabilizing cofactor ring, diminishing or eliminating the possibility of a resonance-stabilized transition state. Although bond reorganization at C-1 of substrate could be occurring concomitant with hydrogen transfer, this would require a contribution of heavy atom movement to the reaction coordinate. Significant movement would appear to be inconsistent with our recent evidence for significant hydrogen tunneling in the BSAO-catalyzed oxidation of benzylamine

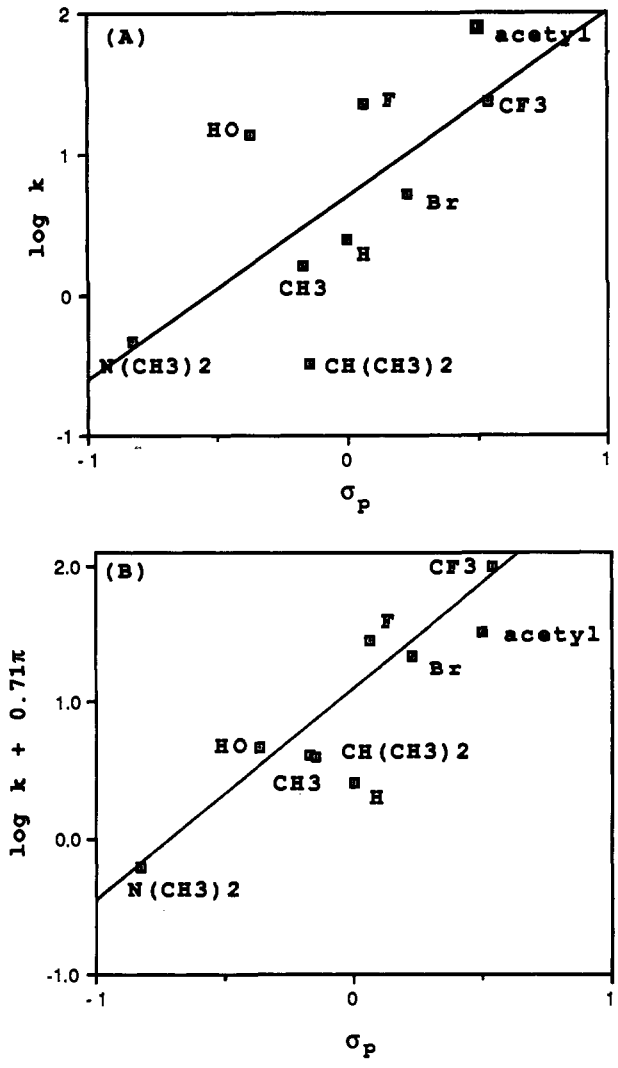

FIGURE 3: Dependence of the rate constant (k_3) for enzyme reduction by para-substituted benzylamine on electron substituent constant (σ_p). (A) Direct correlation of k_3 vs σ_p. (B) Adjusted correlation of $k_3 + 0.71\pi$ vs σ_p. See eq 9 in text.

(Grant & Klinman, 1989). A second argument against the use of the ring oxygen as base comes from the demonstration of a single active site residue catalyzing the oxidation and exchange reactions of phenethylamines (Farnum & Klinman, 1986). Model building experiments, using topa and covalently attached phenethylamine, indicate that steric hindrance would impede catalysis by the oxyanion of cofactor in the hydrogen exchange reaction from the β-carbon of phenethylamine.

Supplementary Material Available

Description of detailed synthesis of isotopically labeled *p*-OH-, *p*-$(CH_3)_2CH$-, and *p*-CH_3CO-benzylamines (the synthesis of these amines required either protection/deprotection steps or synthetic routes different from those outlined under Experimental Procedures) (6 pages). Ordering information is given on any current masthead page.

References

Ameyama, M., Hayashi, U., Matsushita, K., Shinagawa, E., & Adachi, O. (1984) *Agric. Biol. Chem. 48*, 561–565.

Bachrach, U. (1985) in *Structure and Functions of Amine Oxidases* (Mondovi, B., Ed.) pp 5–20, CRC Press, Boca Raton, FL.

Bondi, A. (1964) *J. Phys. Chem. 68*, 441–451.

Buffoni, F. (1966) *Pharmacol. Rev. 18*, 1163–1199.

Cha, Y., Murray, C. J., & Klinman, J. P. (1989) *Science 243*, 1325–1330.

Cleland, W. W. (1979) *Methods Enzymol. 63*, 103–108.

Duine, J. A., Frank, J., & Jongejan, J. A. (1987) *Adv. Enzymol. 59*, 170–212.

Farnum, M. F., & Klinman, J. P. (1986) *Biochemistry 25*, 6028–6036.

Farnum, M., Palcic, M., & Klinman, J. P. (1986) *Biochemistry 25*, 1898–1904.

Grant, K. L., & Klinman, J. P. (1989) *Biochemistry 28*, 6597–6605.

Hartmann, C., & Klinman, J. P. (1987) *J. Biol. Chem. 262*, 962–965.

Janes, S. M., & Klinman, J. P. (1991) *Biochemistry* (preceding paper in this issue).

Janes, S. M., Mu, D., Wemmer, D., Smith, A. J., Kaur, S., Maltby, D., Burlingame, A. L., & Klinman, J. P. (1990) *Science 248*, 981–987.

Klinman, J. P. (1976) *Biochemistry 15*, 2018–2026.

Klinman, J. P., & Matthews, R. G. (1985) *J. Am. Chem. Soc. 107*, 1058–1060.

Klinman, J. P., Hartmann, C., & Janes, S. M. (1988) in *PQQ and Quinoproteins* (Jongejan, J. A., & Duine, J. A., Eds.) pp 297–305, Kluwer, Dordrecht.

Lobenstein-Verbeek, C. L., Jongejan, J. A., Frank, J., & Duine, J. A. (1984) *FEBS Lett. 170*, 305–309.

Lovenberg, W., & Beaven, M. A. (1971) *Biochim. Biophys. Acta 251*, 452–455.

Miller, S., & Klinman, J. P. (1985) *Biochemistry 24*, 2114–2127.

Neumann, R., Hevey, R., & Abeles, R. M. (1975) *J. Biol. Chem. 250*, 6362–6367.

Nystrom, R. G. (1955) *J. Am. Chem. Soc. 77*, 2544–2545.

Palcic, M. M., & Klinman, J. P. (1983) *Biochemistry 22*, 5957–5966.

Ramsey, R. R., Husain, M., & Steenkamp, P. J. (1986) *Biochem. J. 241*, 883–892.

Siegel, R. C. (1979) *Int. Rev. Connect. Tissue Res. 8*, 73–118.

Strickland, S., Palmer, G., & Massey, V. (1975) *J. Biol. Chem. 250*, 4048–4052.

Summers, M. C., Markovic, R., & Klinman, J. P. (1979) *Biochemistry 18*, 1969–1979.

Suva, R. H., & Abeles, R. H. (1978) *Biochemistry 17*, 3538–3545.

Williams, T. J., & Falk, M. C. (1986) *J. Biol. Chem. 261*, 15949–15954.

Yasunobu, K. T., Ishitaki, H., & Minamiura, N. (1976) *Mol. Cell. Biochem. 13*, 5–29.